ORIGINAL RESEARCH PAPER
Volume-8 | Issue-9 | September - 2019 | PRINT ISSN No. 2277 - 8179 | DOI : 10.36106/ijsr
INTERNATIONAL JOURNAL OF SCIENTIFIC RESEARCH

EXPERIMENTAL STUDY BASED ON ACOUSTIC EMISSION AND VIBRATION SIGNALS TO DETECT THE PRESENCE OF DEFECTS IN A ROLLING ELEMENT BEARING

Engineering

Hazim Alsadoon Department of Mechanical Engineering, Gaziantep University, 27310 Gaziantep, Turkey

Sedat Baysec* Department of Mechanical Engineering, Gaziantep University, 27310 Gaziantep, Turkey
*Corresponding Author

Necle Togun Vocational School of Technical Sciences in Gaziantep, University of Gaziantep, 27310 Gaziantep, Turkey

ABSTRACT

In this research, acoustic emission and vibration technology was used to detect defects in the rolling elements bearings, using statistical techniques to analyze the time domain signal. To extract the well-established statistical parameters, Such as the RMS, peak level, crest factor and other features including kurtosis and skewness. This experimental study focused on the analysis of acoustic emission signals and acceleration to determine the presence of defects in the radially loaded bearing. A defect of a certain size was seeded in the inner race and outer race of the test bearings. The results reveal that the AE technology is more effective in detecting bearings faults than that of the vibration measurement, especially in the low frequency range.

KEYWORDS

Acoustic emission, Bearing defect, Vibration, Condition monitoring.

1.INTRODUCTION

The industrial revolution has increased dependence on bearings around the world. Where it has become a common and important element in rotating machines. Therefore, they have received much attention in the area of condition monitoring. Therefore, the condition monitoring system is very useful in the industrial field to determine the state of rotating equipment, to detect any, arising defects to prevent deterioration of machine performance and its evolution into a stage leading to disastrous consequences [1];[2]. Detection of bearing defects can be performed using ultrasonic,

acoustic emission, vibration, oil analysis, stress shape, temperature changes, etc. A common application of fault detection technology is the analysis of acoustic emission and vibration signatures. The sound and vibration monitoring and analysis of rotary machines provide very important information about what is going on inside the metal structure as well as between surfaces that are in contact. This information is useful in assessing the condition of the bearings in order to plan for predictive maintenance [3].

2.Time domain

As a series of digital values, "Vibration signals" can be in a primary manner gathered and it can refer to the velocity, the proximity or even the acceleration in the time-varying plot that can be known as time domain. Moreover, it can help by analyzing or clarifying, as a function of time, the vibration data. The major specialization for the time domain signal format stands for no data or at least a little one that will be lost prior to inspection of vibration signal. A different vibration signature was shown by the vibration signals from a good bearing as well as a faulty bearing even after the energy, elimination, filtering of time domain data and normalization as well [4]. It might be used to analyze failure as well as a fault when the vibration or acoustic data would be analyzed and obtained from the machine component. Widely, the feature extraction and the Statistical methods were utilized to find out the random traits of a vibration signal generated from a physical system. It is clearly that "Feature extraction" that known for the mathematical parameters is by the peaks, randomness and the shape of a time varying signal were represented; moreover, it might be calculated by utilizing higher derivatives of time domain signal. It was proposed by Jens Strackeljan and Tahsin Doguer [5] that "the time domain signal analysis" is applied by what so called "feature extraction of time varying signal" when it concentrates on the properties of a specific part of the time signal; besides, the chosen part might display a close relation to potential bearing defects. By selecting a peak in the time-varying signal, the iteration was done; in addition, in the measured acceleration signal collected from desired rolling element bearing, it could represent the presents of local extreme. Having chosen the local extreme peaks from the time domain signal that improved the demands of the peak definition as well as in a closing manner were relating to the bearing defects, it can be clear that significant information such as adjacent data points, amplitude and peak position, were found to be stored as a time domain vibration signal.

Machine condition monitoring requires an easy-to-interpret and clear condition indicator that can be calculated from the extracted vibration characteristics.Useful indicators should allow for defect growth tracking and provide a way to define indicator levels that indicate acceptable and unacceptable machine conditions [6].

The statistical technique for time domain indicators (RMS, Crest factor, Kurtosis…etc.) associated with a vibration or AE signature of bearings, observed most often in its time domain, are used as condition monitoring indicators for bearing condition., Therefore In this study is focus on the study of the evolution of indicators RMS, CF, skewness, kurtosis, peak value[7].

*2.1*Statistical method

One of the commonly and widely used approaches for analyzing vibrations is statistical approach and the extraction of features through which the characteristics of these signals are studied which are produced by physical systems. Features extraction are mathematical parameters representing the peak, shape and random of the changing signal over time. Statistical indicators (RMS, Crest factor, Kurtosis ...etc.) related to acoustic emission or vibration, Which are extracted from these signals in its temporal waveform, are used in the monitoring of rotating machineries and determine bearings condition.

*2.1.1*Root Mean Square (RMS)

RMS is one of the most common indicators is the RMS (root mean square). Where it has been used in several studies [8].

RMS is possible to quickly check the status of the bearing and also to see if there has been a change in operating conditions since the last measurement. [9].

$$RMS = \sqrt{\frac{1}{N}\sum_{i=1}^{n}(x_i - \mu)2} \qquad (1)$$

*2.1.2*Peak Level

The peak level of the discrete time signal is:

$\text{Peak} = \text{maximum}(x_i)$ (2)

*2.1.3*Crest Factor (CF)

Crest Factor is the ratio of the peak value to the rms value, which consider another factor used as a health indicator that gives a measure for the signal spikiness. [6]

$$CF = \frac{peak \cdot value}{RMS} \qquad (3)$$

*2.1.4*Kurtosis

Kurtosis is an indicator of whether the data is peak or flat relative to the normal distribution. Where high kurtosis value represents the "peak" distribution and the low kurtosis represents the "flat" distribution around the mean. It is very low for healthy bearings and is a high value for defective bearings, because of the spiky behavior for the signal[6]. The mathematical formula for kurtosis is as in equation (4).

$$Kurtosis = \frac{\frac{1}{N}\sum_{i=1}^{n}(x_i - \mu)4}{4} \quad (4)$$

*2.1.5*Skewness

Skewness is a measure of symmetry or, the absence of symmetry relative to its mean value. Where the distribution is symmetry if the left and right points of the distribution center appear identical. Negative skewness values indicate that the data is skewed to the left, and positive values are skewed to the right.

$$Skewness = \frac{\frac{1}{N}\sum_{i=1}^{n}(x_i - \mu)3}{\sigma^3} \quad (5)$$

3.Bearing characteristic frequencies

Periodic pulses produce certain frequencies called characteristic frequencies of defects, occur when a rolling element encounters a defect, These frequencies depend on the geometry and speed of the bearing. as expressed in the following formula[9]:

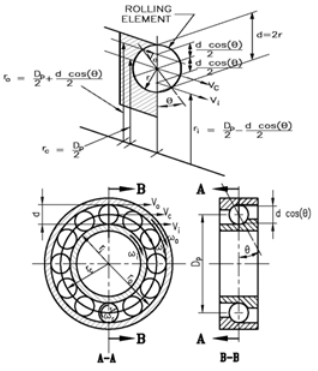

Figure 1: Bearing geometry[27]

Where (f, r, ω, v, θ) refers to frequency, radius, angular speed, linear speed and angular contact of load in radial plane.

Indices: (c, i, r, o) refers to the cage, inner race, rolling element and outer race. (Dp)Pitch diameter ;(d) Diameter of the rolling element ;(Nb) Number of rolling elements.

The linear velocity of the cage can be given as

$$v_c = \frac{v_i + v_o}{2} = \frac{w_i r_i + w_o r_i}{2} = \frac{f_i r_i + f_o r_i}{2} \quad (6)$$

$$r_c = \frac{D_P}{2} \quad (7)$$

$$r_i = \frac{D_P}{2} - \frac{d\cos\theta}{2} \quad (8)$$

$$r_o = \frac{D_P}{2} + \frac{d\cos\theta}{2} \quad (9)$$

Then, the angular speed of cage

$$\omega_c = \frac{v_c}{r_c} \quad (10)$$

$$\omega_c = \frac{1}{2}\left[\omega_i\left(1 - \frac{d\cos\theta}{D_P}\right) + \omega_o\left(1 + \frac{d\cos\theta}{D_P}\right)\right] \quad (11)$$

Where $\omega_c = 2\pi f_c$

Fundamental Train Frequency (FTF) speed can also be obtained from the above equations, as shown

$$FTF = f_c = \frac{1}{2}\left[f_i\left(1 - \frac{d\cos\theta}{D_P}\right) + f_o\left(1 + \frac{d\cos\theta}{D_P}\right)\right] \quad (12)$$

The frequency of passage of the ball in the outer ring (BPFO) can be obtained by multiplying the number of rolling elements (N_b) by the relative angular velocity between the cage and the outer ring.

$$BPFO = N_b(\omega_c - \omega_o) \quad (13)$$

$$= N_b\left[\frac{1}{2}\left\{f_i\left(1 - \frac{d\cos\theta}{D_P}\right) + f_o\left(1 + \frac{d\cos\theta}{D_P}\right)\right\} - f_o\right] \quad (14)$$

Similarly, can obtained the ball pass frequency of inner race (BPFI) by multiplying the number of rolling elements by the relative angular velocity between the cage and the inner ring:

$$BPFI = N_b(\omega_i - \omega_c) \quad (15)$$

$$= f_r = \frac{N_b}{2}(f_i - f_o)\left(1 + \frac{d\cos\theta}{D_P}\right) \quad (16)$$

Frequency of rolling elements rotation around their own axis, called the Ball Spin Frequency (BSF), it can be obtained as shown below:

Taking into account the non-slip of the balls

$$\omega_r = \frac{v_r}{r_r} \quad (17)$$

The tangential velocity of ball at the contact point with the inner race is:

$$v_r = N_b(\omega_i - \omega_c)r_r \quad (18)$$

$$\omega_r = \frac{(\omega_i - \omega_c)}{r_r} r_i \quad (19)$$

$$BSF = f_r = \frac{D_P}{2d}(f_i - f_o)\left[1 - \left(\frac{d\cos\theta}{D_P}\right)^2\right] \quad (20)$$

Since the inner ring is to be the rotating part, it is possible to express mathematically the characteristic frequencies as shown.

$$FTF = f_c = \frac{f_i}{2}\left(1 - \frac{d\cos\theta}{D_P}\right)$$

$$BSF = f_r = \frac{D_P f_i}{2d}\left[1 - \left(\frac{d\cos\theta}{D_P}\right)^2\right]$$

$$BPFI = \frac{N_b f_i}{2}\left(1 + \frac{d\cos\theta}{D_P}\right)$$

$$BPFO = \frac{N_b f_i}{2}\left(1 - \frac{d\cos\theta}{D_P}\right)$$

1.Experimental Setup

For measuring the vibration and AE signature at various loads and speeds, Three levels of load applied on test bearing. The load is applied by using disk load mounted at the free end of the shaft. Split housing is designed for ease of mounting and dismounting the test bearing. Which three single row deep grove ball bearings are used as test bearings with zero contact angle. One of them was without defect as a healthy, the rest were seeded with certain defects at inner and outer raceway. Accelerometer was employed to measure the vibration data, which is stud mounted directly to housing bearing, where is located at the 12 o'clock position of the housing. And free field array microphone to measure the acoustic emission signature. The nature of sound and vibrations to be measured can vary widely. Sound can be “noisy” (roar or hiss-like), which the machine under constant loading emits constant noise, while vibrations of a machine are often dominated by the rotational frequency and its multiples. the defects of the ball bearings in this research is

formed artificially, were created using an electric discharge machine (EDM) of 0.7 mm diameter.

A 4 channel data acquisition unit is used to obtain the vibration and AE signals and the recorded signals are post-processed in Labview environment. The digital data was collected at 1653 samples per second. below schematic diagram of acquisition and processing the data.

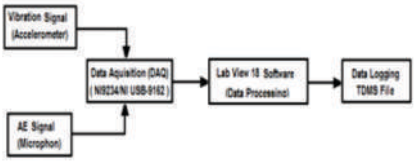

Figure 2: Schematic diagram of acquisition and processing data.

*4.1*Test bench

The test rig used in this study consists of a shaft supported by two Pillow Block Bearing UCP207, which are auto lubricated. connected by flexible coupling to 3 phase induction motor. Four levels of speed

(610, 898, 1224, 1495 rpm) controlled by Powerflex speed variator and three levels of load applied on test bearing using a load disk (0 kg, 5 kg, 10 kg), mounted at the free end of the shaft as in figure x .

The specification and dimension of bearings that used in this test are listed in table 1. And theoretical characteristics frequencies are listed in table 2.

4.2 Instrumentation

The technical specifications of the equipment that used in the collection and analysis of data.

1. General purpose Piezotronics PCB 352C04 accelerometer (10 mV / g).
2. Gras 40PH free field array microphone (50 mV / g).
3. National instrument DAQ 9234 with USB-DAQ9162 chassis.
4. PowerFlex M4 speed variator.

The bearing specifications used in the experiment are as follows: ORS 6206 TN1 C3 (Glass Fibre Reinforced Polyamide 6.6 Plastic Cage)

Table 1: Dimensions of ORS 6206 TN1 C3 bearing

Outer diameter Do	62 mm
Inner diameter Di	30 mm
Width b	16 mm
Ball diameter d	9.52 mm
Pitch diameter	46.5 mm
Contact angle	0
No. of ball	9

Table 2: Theoretical Characteristic defect frequencies at different speeds.

RPM	*610*	*898*	*1224*	*1495*	*Order*
Hz	*10.17*	*14.97*	*20.4*	*24.92*	
FTF	242.55	357.07	486.7	594.46	0.4
	4.04	5.95	8.11	9.9	
BSF	1427.31	2101.19	2863.99	3498.09	2.32
	23.78	35.01	47.73	58.3	
BPFI	3306.98	4868.31	6635.65	8104.82	5.43
	55.11	81.13	110.59	135.08	
BPFO	2183.01	3213.68	4380.34	5350.17	3.57
	36.38	53.56	73	89.16	

Figure 3: Artificial defects on the bearing components

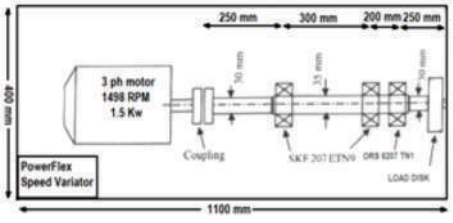

Figure 4: Sketch for test rig.

Figure 5: (a)Test rig (b) housing bearing.

5.RESULTS ANALYSIS AND DISCUSSION

Monitoring the general condition of the bearing can be performed by studying the statistical parameters extracted from the signal in the time domain. Figures 6-17 show the time signal generated from an intact and faulty bearings, respectively.

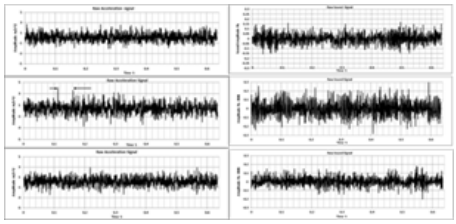

Figure 6: (a) Vibration signature (b) Sound signature at load P0 & 610 rpm (1) Healthy bearing signature (2) Inner race defect signature (3) Outer race defect signature.

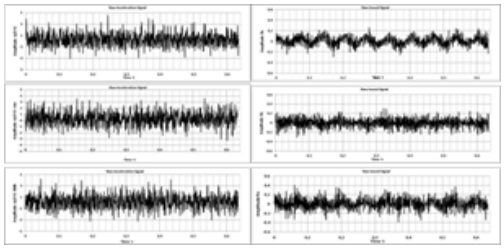

Figure 7: (a) Vibration signature (b) Sound signature at load P0 & 898 rpm (1) Healthy bearing signature (2) Inner race defect signature (3) Outer race defect signature.

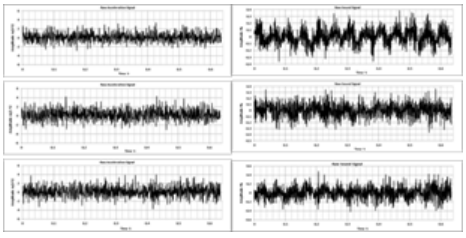

Figure 8: (a) Vibration signature (b) Sound signature at load P0 & 1224 rpm (1) Healthy bearing signature (2) Inner race defect signature (3) Outer race defect signature.

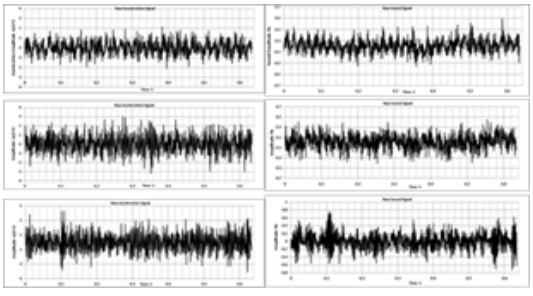

Figure 9: (a) Vibration signature (b) Sound signature at load P0 & 1495 rpm (1) Healthy bearing signature (2) Inner race defect signature (3) Outer race defect signature.

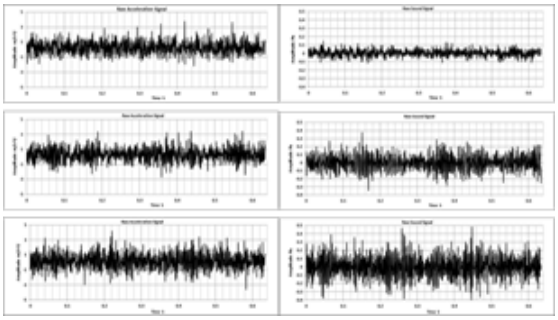

Figure 10: (a) Vibration signature (b) Sound signature at load P1 & 610 rpm (1) Healthy bearing signature (2) Inner race defect signature (3) Outer race defect signature.

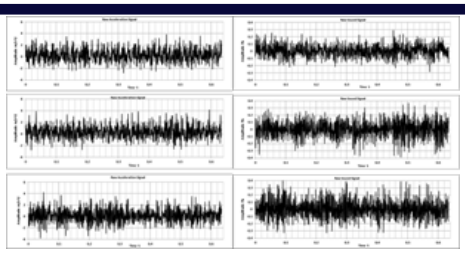

Figure 11: (a) Vibration signature (b) Sound signature at load P1 & 898 rpm (1) Healthy bearing signature (2) Inner race defect signature (3) Outer race defect signature.

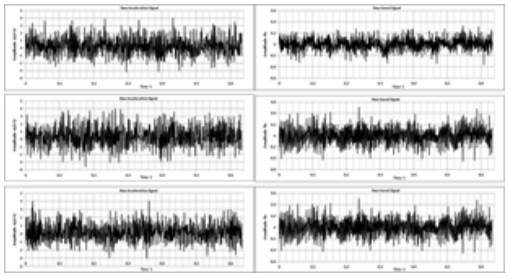

Figure 12: (a) Vibration signature (b) Sound signature at load P1 & 1224 rpm (1) Healthy bearing signature (2) Inner race defect signature (3) Outer race defect signature.

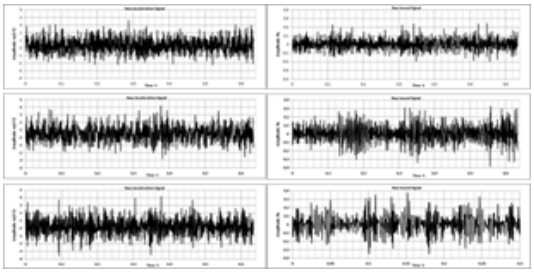

Figure 13: (a) Vibration signature (b) Sound signature at load P1 & 1495 rpm (1) Healthy bearing signature (2) Inner race defect signature (3) Outer race defect signature.

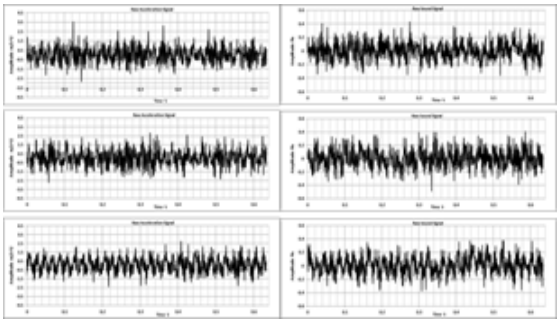

Figure 14: (a) Vibration signature (b) Sound signature at load P2 & 610 rpm (1) Healthy bearing signature (2) Inner race defect signature (3) Outer race defect signature.

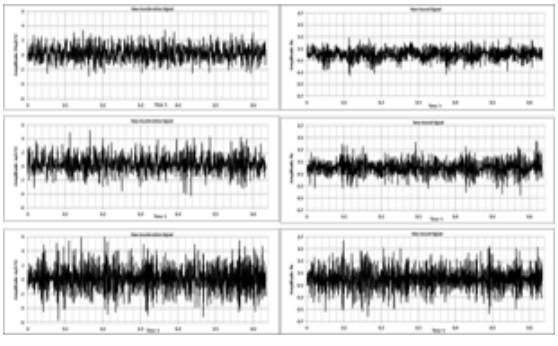

Figure 15: (a) Vibration signature (b) Sound signature at load P2 & 898 rpm (1) Healthy bearing signature (2) Inner race defect signature (3) Outer race defect signature.

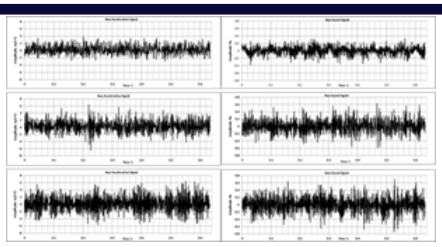

Figure 16: (a) Vibration signature (b) Sound signature at load P2 & 1224 rpm (1) Healthy bearing signature (2) Inner race defect signature (3) Outer race defect signature.

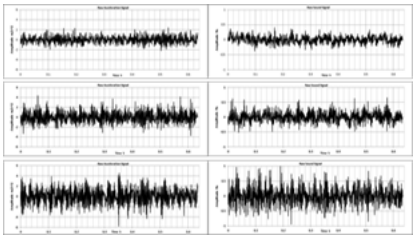

Figure 17: (a) Vibration signature (b) Sound signature at load P2 & 1495 rpm (1) Healthy bearing signature (2) Inner race defect signature (3) Outer race defect signature.

When looking at vibration and sound signals as in figures (6-17) , can be observed a noticeable increase in the signal amplitude of the defective bearings compared with fault-free bearing, and also showed fluctuations and bursts due to defects. Therefore, the waveform signal of the bearing can be considered a quick and initial method of diagnosing the condition of the bearings based on the working history of the bearing.

5.1 RMS feature results

One of the first ways to estimate the level of vibration is the root mean square feature (RMS) of vibration and the AE signal on the bearing housing. Figure 4.29 shows the measured RMS of the Acoustic emission and vibration signals for a fault-free ball bearing and defective bearings over 24 experiments (4 * 2 * 3), where 4 speeds (610 - 898 - 1224 - 1495) rpm. At 3 load levels, which P0, P1 and P2 are denoted as 0 kg, 5.5 kg and 10 kg respectively for two defects in different places. The root-mean-square value of vibration signals is presented depending on each experiment with a different speeds and loads.

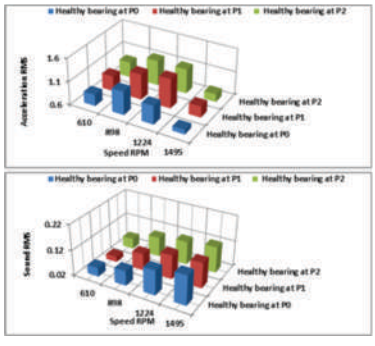

Figure 18: RMS value for Healthy case signature at deferent load (a) Acceleration signal RMS (b) Sound signal RMS.

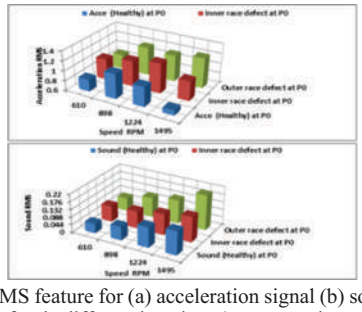

Figure 19: RMS feature for (a) acceleration signal (b) sound signal at load P0 and defect in different locations (outer race, inner race).

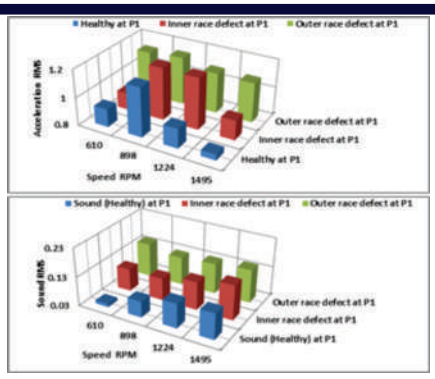

Figure 20: RMS feature for (a) acceleration signal (b) sound signal at load P1 and defect in different locations (outer race, inner race).

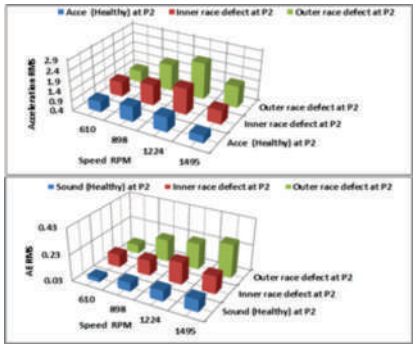

Figure 21: RMS feature for (a) acceleration signal (b) sound signal at load P2 and defect in different locations (outer race, inner race).

Figures 19-21 show that the RMS value of the AE signature is a good indicator of fault monitoring in all cases, and the RMS value of the acceleration signature is also a good indicator, except for the low frequency range of the inner ring defect feature, where the value decreases below the RMS of the health case as shown in Figure 20a.

5.2 Crest factor result

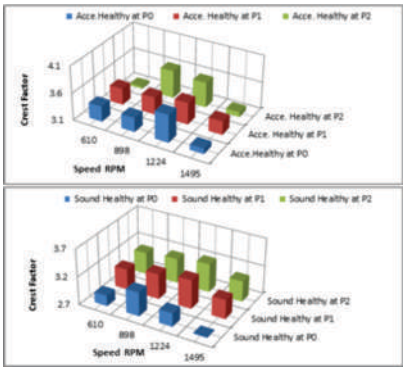

Figure 22: Crest factors for Healthy case signature at deferent load (a) Acceleration Crest Factors (b) Sound Crest Factors.

Figure 22 shows that the acoustic emission signal and vibration signal increases with increasing load and speed, but decreases after 1224 rpm at all loads.

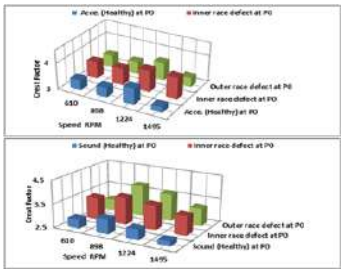

Figure 23: Crest factors feature for (a) acceleration signal (b) sound signal at load P0 and defects in different locations.

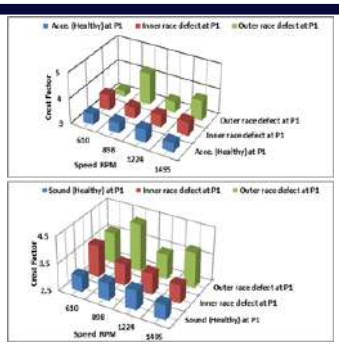

Figure 24: Crest factors feature for (a) acceleration signal (b) sound signal at load P1 and defects in different locations.

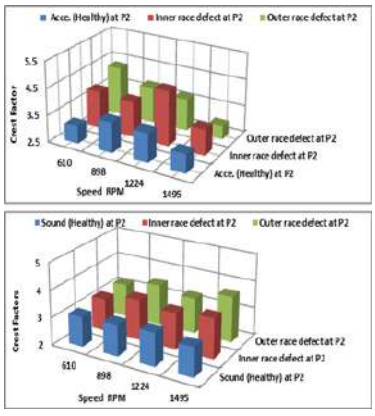

Figure 25: Crest factors feature for (a) acceleration signal (b) sound signal at load P2 and defects in different locations.

Figure 23-25 shows that the acoustic emission crest factor is a good indicator of bearing defects. Defective bearings can be easily identified at all loads and speeds. Although the acceleration signal crest factor clearly indicates the defect only at the P0 load level, there are no significant bearing defect indications at loads P1 and P2, except at some relatively low and medium speeds.

5.3 The skewness results

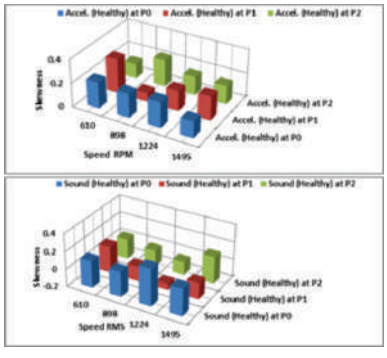

Figure 26: Skewness feature for Healthy case signature at deferent load (a) Acceleration Skewness (b) Sound Skewness

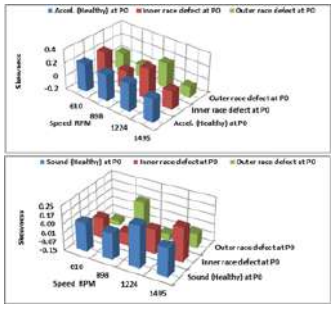

Figure 27: Skewness feature for (a) acceleration signal (b) sound signal at load P0 and defects in different locations.

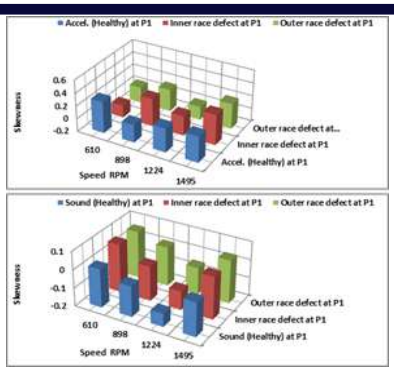

Figure 28: Skewness feature for (a) acceleration signal (b) sound signal at load P1 and defects in different locations.

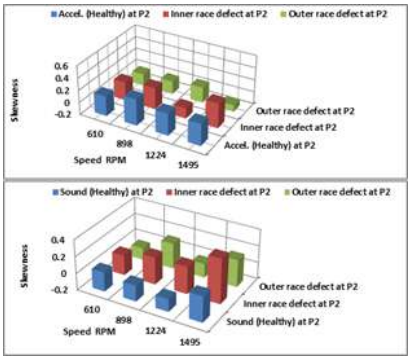

Figure 29: Skewness feature for (a) acceleration signal (b) sound signal at load P2 and defects in different locations.

Figures 27-29 show that the skewness of the sound signal indicates a defect in the bearing when the load is increased to levels P1 and P2, and it does not indicate a fault in the load level P0. For acceleration signal, the skewness feature failed to identify any defects in the experiments, except of a limited cases, at a certain speed in the case of bearing with defective inner rings.

5.4 The kurtosis results

A signal with a Gaussian distribution has a kurtosis value equivalent to 3. But as the fault occurs on the ball bearings, the signal becomes noisy, the distribution changes, and the kurtosis characteristic value is higher than 3[11].

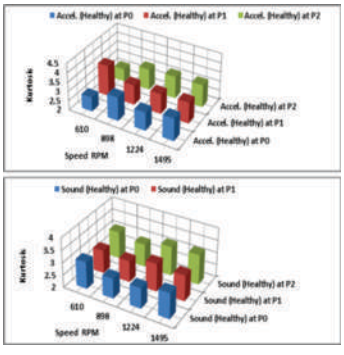

Figure 30: Kurtosis feature for Healthy case signature at deferent load (a) Acceleration Kurtosis (b) Sound Kurtosis.

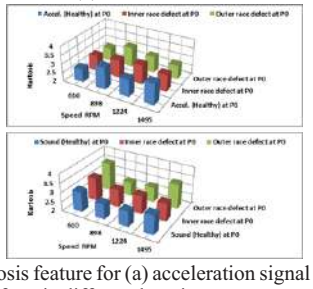

Figure 31: Kurtosis feature for (a) acceleration signal (b) sound signal at load P0 and defects in different locations.

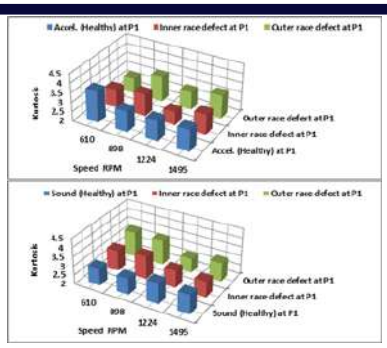

Figure 32: Kurtosis feature for (a) acceleration signal (b) sound signal at load P1 and defects in different locations.

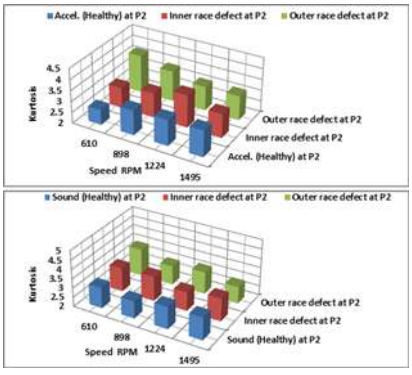

Figure 33: Kurtosis feature for (a) acceleration signal (b) sound signal at load P2 and defects in different locations.

As shown in Figures 30-33, the kurtosis feature of the AE signal indicate a significant increase in amplitude at low speed range (610 rpm and 898 rpm) for all bearing defects and a random increase at high speed. Localized defects in the bearing increase the pulse content of the signal; therefore, the kurtosis value as a measure of the peak waveform will also increase. A healthy bearing signal exhibits an ideal Gaussian behavior in the time domain, so the kurtosis feature value of a free-fault bearing should be around 3 [11], [12]. At speeds of 612 and 898 rpm, the kurtosis value of a defective bearings exceeds 3, at all loads. This is a good indication of faults at the low speeds. The kurtosis of the vibration acceleration signal is an important statistical parameter of the signal behavior, but does not reflect the obvious degradation trend of the bearing condition in this study.

5.5 Peak level results

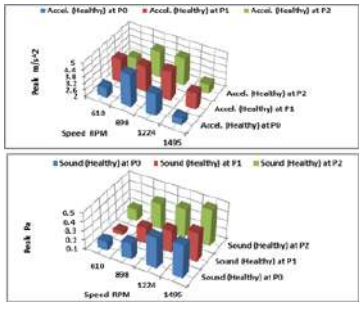

Figure 34: Peak feature for Healthy case signature at deferent load (a) Acceleration Peak value (b) Sound Peak.

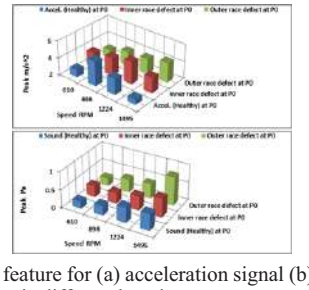

Figure 35: Peak feature for (a) acceleration signal (b) sound signal at load P0 and defects in different locations.

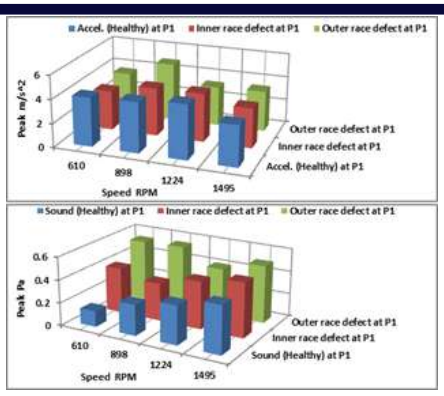

Figure 36: Peak feature for (a) acceleration signal (b) sound signal at load P1 and defects in different locations.

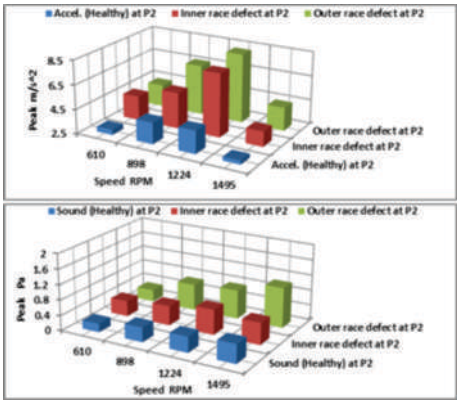

Figure 37: Peak feature for (a) acceleration signal (b) sound signal at load P2 and defects in different locations.

At P0 load, the peak feature of the acceleration signal show interesting results only at high speeds, while the peak feature of the acoustic signal show a reliable indication of bearing failure at all speeds and in all cases, except at the speed of 1224 rpm. However, as the load increases to the P 1 and P 2 levels, the peak increases, confirming that there is a clear indication of bearing defects. Thus, the peak feature of acceleration and acoustic emission signals, is a good indicator of bearing defects, but the AE peak is better and more obvious than the acceleration peak characteristic, as shown in Figures (35-37).

3.CONCLUSION

Acoustic emission technology is as good as vibration measurement for detecting bearing defects. More specifically, acoustic emission is more sensitive than vibration technique in all frequency bands of this study, especially in the low frequency band, which is very effective in detecting initial failures by statistically analyzing signals to extract appropriate features.

In summary, we can conclude that there is an integration between these technologies to monitor bearing condition and diagnose defects over a wide range of speeds.

4.REFERENCES

[1] Mohanty, S. (2016). Vibro Acoustic Health Monitoring of Bearing using Signal Processing Techniques.
[2] Manohar, V. G., & Cumar, P. (2003). Comprehensive Predictive Maintenance of Electrical Motors in Indian Nuclear Power Plants. Nu-Power, 17, 1-3.
[3] Tandon, N., & Choudhury, A. (1999). A review of vibration and acoustic measurement methods for the detection of defects in rolling element bearings. Tribology international, 32(8), 469-480.
[4] Eric Y. Kim, Andy C. C. Tan, Bo-Suk Yang and Vladis Kosse, "Experimental Study on Condition Monitoring of Low Speed Bearings: Time Domain Analysis," 5th Australasian Congress on Applied Mechanics, ACAM 2007 10-12 December 2007, Brisbane, Australia
[5] Tahsin Doguer and Jens Strackeljan, "Vibration analysis using time domain methods for the detection of small roller Bearing Defects," SIRM 2009 - 8th International conference on vibrations in rotating machines, Vienna, Austria, 23 - 25 February 2009
[6] Bhende, A. R., Awari, G. K., & Untawale, S. P. (2014). Comprehensive bearing condition monitoring algorithm for incipient fault detection using acoustic emission. Jurnal Tribologi, 2, 1-30.
[7] El Anouar, B. A., Elamrani, M., Elkihel, B., Delaunois, F., & Manssouri, I. (2017). A comparative experimental study of different methods in detection and monitoring bearing defects. International Journal of Advanced Scientific and Technical Research, (7). [4] Roque, A.
[8] Mathew, J., & Alfredson, R. J. (1984). The condition monitoring of rolling element bearings using vibration analysis. Journal of vibration, acoustics, stress, and reliability in design, 106(3), 447-453.
[9] El Anouar, B. A., Elamrani, M., Elkihel, B., Delaunois, F., & Manssouri, I. (2017). A comparative experimental study of different methods in detection and monitoring bearing defects. International Journal of Advanced Scientific and Technical Research, (7).
[10] A., Silva, T. A. N., & Dias, J. C. Q. (2009). An approach to fault diagnosis of rolling bearings. WSEAS transactions on systems and control, (4), 4.J. Geralds,
[11] Mobley, R. K. (1999). Vibration fundamentals. Elsevier.
[12] Roque, A. A., Silva, T. A. N., & Dias, J. C. Q. (2009). An approach to fault diagnosis of rolling bearings. WSEAS transactions on systems and control, (4), 4.